J|A|C|S ARTICLES

Published on Web 09/25/2009

Morphology and Melting Behavior of Ionic Liquids inside Single-Walled Carbon Nanotubes

Shimou Chen,[†] Keita Kobayashi,[†] Yasumitsu Miyata,[†] Naoki Imazu,[†] Takeshi Saito,[‡,§] Ryo Kitaura,[†] and Hisanori Shinohara*[,†]

Department of Chemistry and Institute for Advanced Research, Nagoya University, Nagoya, 464-8602, Japan, Nanotube Research Center, National Institute of Advanced Industrial Science and Technology, Tsukuba 305-8565, Japan, and PRESTO, Japan Science and Technology Agency, 4-1-8 Honcho Kawaguchi, Saitama, Japan

Received May 26, 2009; E-mail: noris@nagoya-u.jp

Abstract: We report the synthesis and characterization of single-walled carbon nanotubes (SWNTs) filled with a zinc-containing quaternary ammonium based ionic liquid ($ChZnCl_3$) inside. The threshold SWNT diameter for efficient encapsulation was determined to be ca. 0.97 nm. Different morphologies of the encapsulated $ChZnCl_3$ such as single-chain, double-helix, zigzag tubes, and random tubes were observed. The melting of $ChZnCl_3$ ionic liquid into "nanofluid" inside SWNTs was investigated by *in situ* TEM electron beam irradiation and compared with a high-temperature heat treatment. The thermal-decomposition temperature of the $ChZnCl_3$ ionic liquid confined in the SWNTs was much higher than in the bulk system. Furthermore, the doping effect of the encapsulated $ChZnCl_3$ on the host SWNTs can be varied (from p-type to n-type) by gradually reducing the filling ratio. The versatility of ionic liquids and the unique phase transition observed inside the SWNTs provide a new opportunity for modulating the electronic properties of carbon nanotubes.

1. Introduction

Room temperature ionic liquids (RTILs) have received much attention during the past decade due to their unique structural and intermediate phase properties.[1−3] The physical and chemical properties of RTILs have been extensively studied by experimental and theoretical methods.[4−8] Obtaining a molecular-based understanding of the microstructure and morphology of RTILs remains a great challenge due to the complex interplay of molecular interactions. Many RTILs exhibit structural heterogeneities and microphase-separation at the nanometer scale in bulk liquid and supercooled states.[9−11] However, little is understood about the morphology and phase behavior of RTILs in nanometer-scale confinement.[6,12] In a confined space, crystal structures conspire with additional quantum mechanical effects to modulate material properties. The morphology of RTILs is therefore determined not only by interatomic and intermolecular interactions but also by self-imposed surface energy and externally applied geometrical constraints.[13]

The effect of confinement within carbon nanotubes (CNTs) on molecular packing, motion, and reactivity has been investigated by a number of researchers during the past decade.[14] It has been shown that the restricted, one-dimensional space of CNTs can regulate the growth behavior of encapsulated materials in a very precise fashion.[15] Compared with water and other traditional solvents, typical RTILs also consist of a hydrogen bond network and are not simple fluids: their ions are generally asymmetric and flexible with delocalized electrostatic charges. Other sophisticated interactions present in RTILs, such as Coulombic forces, van der Waals forces, polarization, and hydrogen bonding, make their phase transition processes more complex than those of other fluids.[3,16,17]

The study of ionic liquids in a confined state presents an exciting challenge and is of importance in practical applications. The understanding of the morphology and phase behavior of confined RTILs has attracted great attention due to their

[†] Nagoya University.
[‡] National Institute of Advanced Industrial Science and Technology.
[§] Japan Science and Technology Agency.

(1) Binnemans, K. *Chem. Rev.* **2005**, *105*, 4148–4204.
(2) Wang, Y.; Jiang, W.; Yan, T.; Voth, G. A. *Acc. Chem. Res.* **2007**, *40*, 1193–1199.
(3) Weingrtner, H. *Angew. Chem., Int. Ed.* **2008**, *47*, 654–670.
(4) Castner, E. W.; Wishart, J. F.; Shirota, H. *Acc. Chem. Res.* **2007**, *40*, 1217–1227.
(5) Hu, Z.; Margulis, C. J. *Acc. Chem. Res.* **2007**, *40*, 1097–1105.
(6) Lynden-Bell, R. M.; Pópolo, M. G. D.; Youngs, T. G. A.; Kohanoff, J.; Hanke, C. G.; Harper, J. B.; Pinilla, C. C. *Acc. Chem. Res.* **2007**, *40*, 1138–1145.
(7) Iwata, K.; Okajima, H.; Saha, S.; Hamaguchi, H. *Acc. Chem. Res.* **2007**, *40*, 1174–1181.
(8) Smiglak, M.; Metlen, A.; Rogers, R. D. *Acc. Chem. Res.* **2007**, *40*, 1182–1192.
(9) Atkin, R.; Warr, G. G. *J. Phys. Chem. B* **2008**, *112*, 4164–4166.
(10) Triolo, A.; Russina, O.; Fazio, B.; Triolo, R.; Cola, E. D. *Chem. Phys. Lett.* **2008**, *457*, 362–365.
(11) Triolo, A.; Russina, O.; Bleif, H.-J.; Cola, E. D. *J. Phys. Chem. B* **2007**, *111*, 4641–4644.
(12) Park, H. S.; Choi, Y. S.; Jung, Y. M.; Hong, W. H. *J. Am. Chem. Soc.* **2008**, *130*, 845–852.
(13) Mickelson, W.; Aloni, S.; Han, W.; Cumings, J.; Zettl, A. *Science* **2003**, *300*, 467–469.
(14) Khlobystov, A. N.; Britz, D. A.; Briggs, G. A. D. *Acc. Chem. Res.* **2005**, *38*, 901–909.
(15) Kitaura, R.; Shinohara, H. *Chem. Asian J.* **2006**, *1*, 646–655.
(16) Maginn, E. J. *Acc. Chem. Res.* **2007**, *40*, 1200–1207.
(17) Dupont, J. *J. Braz. Chem. Soc.* **2004**, *15*, 341–350.

10.1021/ja904283d CCC: $40.75

relevance in catalytic processes, lubricants, nanocomposites, fuels, and solar cells.[18−32] For example, Kanakubo and coworkers[22] reported an intriguing melting-point-depression of 1,3-dialkylimidazolium-based ionic liquids confined in controlled-pore glasses. Néouze et al.[24] found that when $BMINO_3$ was entrapped by silver nanoparticles, the thermal stability of the ionic liquid in the composite became much higher than that of the neat $BMINO_3$. In addition to these studies, Sha et al.[31] reported a drastic phase transition in [Dmim][Cl] ionic liquid confined between two graphene walls. In our previous work,[32] we also found a transition of [bmim][PF_6] from liquid to a high-melting-point crystal when it was confined in multiwalled CNTs. However, a detailed study of the microstructure of RTILs confined in carbon nanotubes has yet to be reported.

High-resolution transmission electron microscopy (HRTEM) can directly determine the packing configurations and morphology transformation of materials in nanospace and has the potential to be a powerful technique for understanding the behavior of RTILs under nanoconfinment. Furthermore, as RTILs have essentially zero vapor pressure and a high thermal and radiation stability they are excellent models for studying "nanofluids" in microscopic detail. In addition to serving as a model, the encapsulation of RTILs inside CNTs may provide a new route for modulating the electronic properties of nanotubes. This could be achieved through the doping effect, which may be tuned by choosing a specific combination of cations and anions among the numerous possibilities (there are claimed to be over 10^{18} possible combinations in ionic liquids[33]). Although the electronic properties of CNTs affected by surface modification or electrochemical doping of RTILs have been investigated by several research groups,[34−38] the doping effect of CNTs filled with RTILs in their hollow interior remains unexplored.

Using HRTEM, we report here the formation of different stacking configurations (including single-chain, double-helix, zigzag tubes and random tubes) of RTILs inside single-walled carbon nanotubes (SWNTs). This series of ordered ionic liquid structures were observed in one-dimensional confinement for the first time. By using the electron beam radiation of TEM together with normal heat-treatment, we were able to observe the melting process of the tubular ionic liquid. In addition, the doping effect of the encapsulated RTILs was investigated by using Raman spectroscopy.

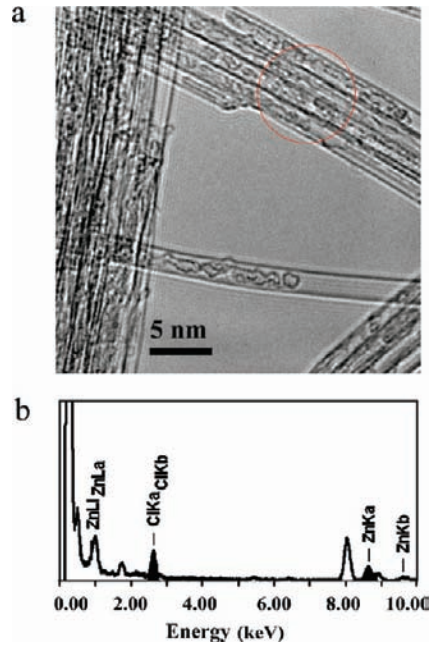

Figure 1. (a) Typical TEM image of $ChZnCl_3$@SWNTs and (b) the corresponding EDX spectrum taken from within the circled area.

2. Results and Discussion

2.1. Encapsulation of Ionic Liquids Inside SWNTs. A zinc-containing quaternary ammonium based ionic liquid $[Me_3NC_2H_4OH]^+[ZnCl_3]^-$ (hereafter referred to as $ChZnCl_3$) was chosen to achieve a high resolution and contrast for TEM imaging. When the $ChZnCl_3$ encapsulated in SWNTs (referred to as $ChZnCl_3$@SWNTs) was examined by TEM, some thin-inner tubes and linear aggregates were clearly observed inside the SWNTs, and virtually no ionic liquids were seen on the outer surface of the SWNTs (Figure 1a). Extensive examination of TEM micrographs revealed that the filling ratio for the $ChZnCl_3$ was as high as 80%. From the energy dispersive X-ray (EDX) spectrum taken for the $ChZnCl_3$@SWNTs (Figure 1b), the peaks at 2.62 and 8.63 keV can be assigned to ClKα and ZnKα, respectively, which confirms the existence of $ChZnCl_3$ within the SWNTs. The X-ray diffraction (XRD) pattern of $ChZnCl_3$@SWNTs shows a significant reduction of the characteristic (10) diffraction peak of the two-dimensional triangular lattice of SWNT bundles, which is consistent with the high filling ratio estimated by the TEM observations (cf. Supporting Information, Figure S1).[39]

The encapsulation of atoms/molecules often quenches the photoluminescence (PL) of SWNTs or induces spectral shifts of emission lines, which is generally attributed to the formation of localized hybridized states between the valence and conduc-

(18) Baldelli, S. *Acc. Chem. Res.* **2008**, *41*, 421–431.
(19) Xu, W.; Angell, C. A. *Science* **2003**, *302*, 422–425.
(20) Fukushima, T.; Kosaka, A.; Ishimura, Y.; Yamamoto, T.; Takigawa, T.; Ishii, N.; Aida, T. *Science* **2003**, *300*, 2072–2074.
(21) Kuang, D.; Ito, S.; Wenger, B.; Klein, C.; Moser Jacques, E.; Humphry-Baker, R.; Zakeeruddin Shaik, M.; Gratzel, M. *J. Am. Chem. Soc.* **2006**, *128*, 4146–4154.
(22) Kanakubo, M.; Hiejima, Y.; Minami, K.; Aizawa, T.; Nanjo, H. *Chem. Commun.* **2006**, 1828–1830.
(23) Néouze, M.; Bideau, J. L.; Gaveau, P.; Bellayer, S.; Vioux, A. *Chem. Mater.* **2006**, *18*, 3931–3936.
(24) Néouze, M.; Litschauer, M. *J. Phys. Chem. B* **2008**, *112*, 16721–16725.
(25) Shimano, S.; Zhou, H.; Honma, I. *Chem. Mater.* **2007**, *19*, 5216–5221.
(26) Atkin, R.; Warr, G. G. *J. Phys. Chem. C* **2007**, *111*, 5162–5168.
(27) Lunstroot, K.; Driesen, K.; Nockemann, P.; Gorller-Walrand, C.; Binnemans, K.; Bellayer, S.; Bideau, J. L.; Vioux, A. *Chem. Mater.* **2006**, *18*, 5711–5715.
(28) Hanabusa, K.; Fukui, H.; Suzuki, M.; Shirai, H. *Langmuir* **2005**, *21*, 10383–10390.
(29) Pinilla, C.; Pópolo, M. G. D.; Lynden-Bell, R. M.; Kohanoff, J. *J. Phys. Chem. B* **2005**, *109*, 17922–17927.
(30) Sha, M.; Wu, G.; Fang, H.; Zhu, G.; Liu, Y. *J. Phys. Chem. C* **2008**, *112*, 18584–18587.
(31) Sha, M.; Wu, G.; Liu, Y; Tang, Z.; Fang, H. *J. Phys. Chem. C* **2009**, *113*, 4618–4622.
(32) Chen, S.; Wu, G.; Sha, M.; Huang, S. *J. Am. Chem. Soc.* **2007**, *129*, 2416–2417.
(33) Rogers, R. D.; Seddon, K. R. *Science* **2003**, *302*, 792–793.
(34) Fukushima, T.; Aida, T. *Chem.—Eur. J.* **2007**, *13*, 5048–5058.
(35) Wang, J.; Chu, H.; Li, Y. *ACS Nano* **2008**, *2*, 2540–2546.
(36) Lpez-Pastor, M.; Domnguez-Vidal, A.; Ayora-Caada, M. J.; Simonet, B. M.; Lendl, B.; Valcrcel, M. *Anal. Chem.* **2008**, *80*, 2672–2679.
(37) Kavan, L.; Kalbáč, M.; Zukalová, M.; Dunsch, L. *Carbon* **2006**, *44*, 99–106.
(38) Kavan, L.; Dunsch, L. *ChemPhysChem* **2003**, *4*, 944–950.
(39) Cambedouzou, J.; Pichot, V.; Rols, S.; Launois, P.; Petit, P.; Klement, R.; Kataura, H.; Almairac, R. *Eur. Phys. J., B* **2004**, *42*, 31–45.

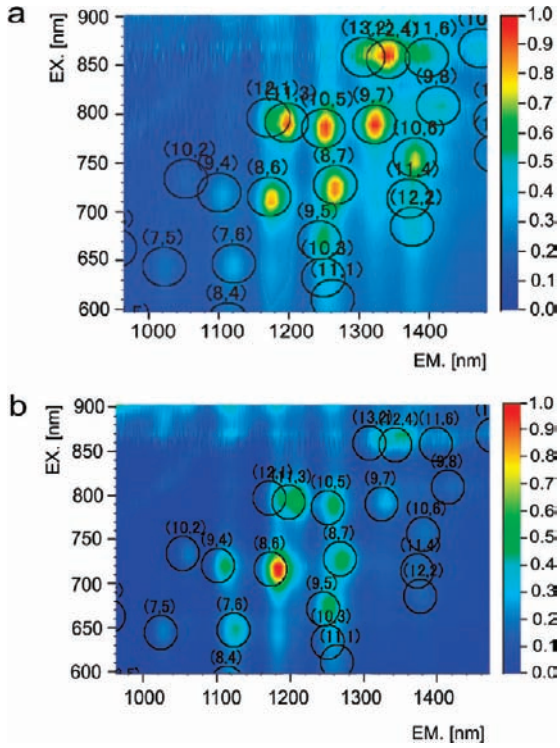

Figure 2. Two-dimensional contour plots of the NIR photoluminescence of (a) SWNTs/SDBS/D_2O (pH = 7.8) and (b) $ChZnCl_3$@SWNTs /SDBS/D_2O (pH = 7.8).

tion bands of nanotubes.[40] The qualitative threshold value for filling can be obtained by comparing the emission intensities derived from filled and unfilled tubes treated by a similar process. We therefore measured the two-dimensional contour plots of the PL of SWNTs and $ChZnCl_3$@SWNTs dispersed by dodecylbenzene sulfonate (SDBS) in D_2O (Figure 2). Our results indicate that the main species in the pristine SWNTs are those having the chiralities of (8, 6), (11, 3), (8, 7), (10, 5), (9, 7), (12, 4), and (11, 4) (Figure 2a). However, the major PL emitting species for $ChZnCl_3$@SWNTs stems from (8, 6), and the intensities of the other thick tubes such as (11, 3), (8, 7) and (10, 5) were reduced remarkably (Figure 2b), suggesting that there is a threshold value in the nanotube diameter for the filling process. In order to investigate the diameter-selective encapsulation in detail, the relative PL intensities of SWNTs and $ChZnCl_3$@SWNTs were plotted as a function of tube diameter (Figure 3). A drastic decrease in the PL intensity of $ChZnCl_3$@SWNTs was observed at a diameter of ~0.97 nm. The sudden reduction of PL intensities observed at diameters of 0.97−1.10 nm suggests the encapsulation of $ChZnCl_3$ and a charge-transfer event occurring between the encapsulated $ChZnCl_3$ and the nanotubes.[41−43]

For the SWNTs having tube diameters of >1.10 nm, the PL intensity of $ChZnCl_3$@SWNTs was similar to that of the pristine SWNTs. In these large diameter SWNTs, the encapsulated

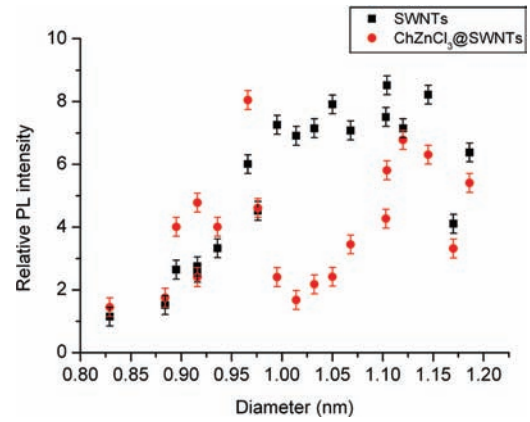

Figure 3. Relative photoluminescence intensity of pristine SWNTs (black squares) and $ChZnCl_3$@SWNTs (red circles) as a function of nanotube diameter.

$ChZnCl_3$ can easily dissolve out of the tubes in D_2O (water is a good solvent for $ChZnCl_3$). Based on the PL analysis, the $ChZnCl_3$ could only be encapsulated by those SWNTs having diameters larger than ~0.97 nm. This threshold value agrees well with a theoretical calculation. The van der Waals surface of $ChZnCl_3$ can be approximated by a sphere of 0.7 nm in diameter, as determined from the bond lengths and van der Waals radii of the atoms constituting $ChZnCl_3$.[44] As the van der Waals radius of an sp^2-bonded carbon in the nanotube walls is ~0.15 nm,[45] the smallest tube diameter capable of being filled by $ChZnCl_3$ should be approximately 1 nm (= 0.7 nm + 2 × 0.15 nm).

2.2. Size-Dependent Morphology of Ionic Liquid Inside SWNTs. The packing arrangement of C_{60} molecules in SWNTs is known to depend on the nanotube diameter.[14] Likewise, we expected that different morphologies of $ChZnCl_3$ would be formed in the SWNTs of different diameters. By successively increasing the nanotube diameter from 1.2 to 2.1 nm, the $ChZnCl_3$ patterns varied from single-chain, double-helix, zigzag tube, and random tubular forms (Figure 4), demonstrating that the configuration of the $ChZnCl_3$ depends on the nanotube diameter. The resulting $ChZnCl_3$ morphologies generally displayed structural characteristics not present in their bulk and film forms. This is a clear manifestation of the confinement effect of ionic liquids in SWNTs.

On the basis of the observed TEM images, we constructed a series of structural models for $ChZnCl_3$ inside the SWNTs (Figure 4, center). For each model, the simulated annealing calculation was applied to find the optimum structure with the lowest Coulombic potential energy. Using the constructed models, HRTEM image simulation by the multislice method was performed (Figure 4, right side). The simulated HRTEM images agree well with the four different morphologies of the encapsulated $ChZnCl_3$ ionic liquid.

With respect to the molecules inside thin-diameter SWNTs, similar single-chain and double-helix morphologies of C_{60} have been observed in C_{60}@SWNT peapods, which can be explained by the hard sphere packing in a minimum-energy configuration inside the hard cylindrical cavity.[13,14] Sha et al.[30,31] predicated

(40) Okazaki, T.; Okubo, S.; Nakanishi, T.; Joung, S.; Saito, T.; Otani, M.; Okada, S.; Bandow, S.; Iijima, S. *J. Am. Chem. Soc.* **2008**, *130*, 4122–4128.
(41) Dukovic, G.; White, B. E.; Zhou, Z.; Wang, F.; Jockusch, S.; Steigerwald, M. L.; Heinz, T. F.; Friesner, R. A.; Turro, N. J.; Brus, L. E. *J. Am. Chem. Soc.* **2004**, *126*, 15269–15276.
(42) Paul, A.; Samanta, A. *J. Phys. Chem. B* **2007**, *111*, 1957–1962.
(43) Blesic, M.; Lopes, A.; Melo, E.; Petrovski, Z.; Plechkova, N. V.; Canongia Lopes, J. N.; Seddon, K. R.; Rebelo, L. P. N. *J. Phys. Chem. B* **2008**, *112*, 8645–8650.
(44) Zhong, C.; Sasaki, T.; Jimbo-Kobayashi, A.; Fujiwara, E.; Kobayashi, A.; Tada, M.; Iwasawa, Y. *Bull. Chem. Soc. Jpn.* **2007**, *80*, 2365–2374.
(45) Li, L.; Khlobysto, A. N.; Wiltshire, J. G.; Briggs, G. A. D.; Nicholas, D. R. J. *Nat. Mater.* **2005**, *4*, 481–485.

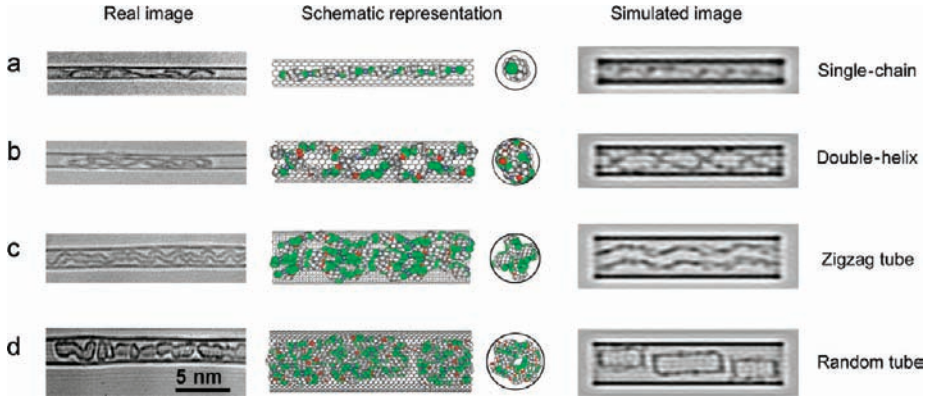

Figure 4. Packing arrangement of $ChZnCl_3$ inside SWNTs of different nanotube diameters. The observed (left side) and simulated (right side) HRTEM images of four typical morphologies of $ChZnCl_3$ ((a)single-chain, (b) double-helix, (c) zigzag tubes, and (d) random tubes) are shown. On the basis of the TEM images, structural models (center) were constructed and the diameter of the SWNTs suitable for each configuration were determined (center right). The calculated tube diameters for the single-chain, double-helix, zigzag tubes, and random sizes are 1.2, 1.4, 1.8 and 2.1 nm, respectively.

theoretically the formation of solid monolayer [Dmim][Cl] ionic liquids when they are confined between two parallel graphene walls. In the present case, the inner surface of SWNTs can also provide a similar interfacial confinement effect as mentioned above, in which the $ChZnCl_3$ assemble into a contact layer with a preference for orientation. Such interfacial-induced solidification together with nanosized confinement effects cause the $ChZnCl_3$ molecules to assemble together and when the diameter is suitable, fold into a cylindrical sheet inside the SWNTs. This results in the formation of an inner $ChZnCl_3$ nanotube.

2.3. Melting Behavior of Confined Ionic Liquid. The transformation and reaction of fullerene chains in SWNT peapods via TEM electron beam irradiation has been studied by many research groups.[46] As the "knock-on damage threshold" for CNTs is low, structural damage can easily be induced by using an accelerating energy of 97−120 kV during HRTEM obersvation.[47] Here, we demonstrate that the $ChZnCl_3$ ionic liquid nanotubes could be melted to generate "nanofluids" by exposing the $ChZnCl_3$@SWNTs to electron beam irradiation with an accelerating voltage of 80 kV. At this voltage, the applied electron beam was high enough to distort the $ChZnCl_3$ nanostructure but not so high as to damage the SWNTs.[47,48]

Using TEM, a section of $ChZnCl_3$@SWNT was subjected to continuous electron beam radiation during which a series of TEM images were taken (Figure 5). At the start of irradiation (Figure 5a), the random tubes of $ChZnCl_3$ were separately loaded inside the SWNTs. As time progressed, the tubes slowly fused to form a zigzag tube (Figure 5c) which exhibited a morphology similar to the $ChZnCl_3$ confined in the SWNTs with a diameter of 1.8 nm (Figure 4c). This indicates that the morphology of confined $ChZnCl_3$ is sensitive to irradiation. After 10 min of electron beam irradiation, the random tubes transformed into a continuous tubular structure (Figure 5a−e). The transformation process could be divided into two steps: (1) the separated $ChZnCl_3$ nanotubes exhibited a corkscrew rotation and assembled together, and then (2) the solid-like state of $ChZnCl_3$ transformed into a liquid-like state and assembled into a contact layer on the inner surface of the SWNTs. Further electron beam irradiation led to the collapse of the tubular structure (Figure 5i−l), and the liquid-like behavior of $ChZnCl_3$ could be distinguished by the free movement of a nanobubble (as indicated by the arrow in Figure 5j). (cf. Supporting Information, Figure S2).

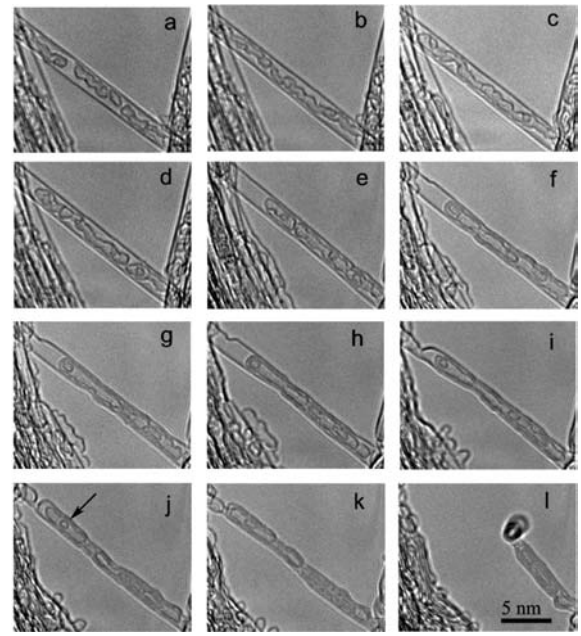

Figure 5. Time sequence (a−l) of TEM images of $ChZnCl_3$@SWNTs showing the melting of $ChZnCl_3$ nanotubes into nanofluids inside SWNTs. Images were taken every 2 min, over a period of 22 min. The arrow in j indicates a nanobubble.

Due to the high thermal stability and wide-range of the liquid state, the nanofluids of $ChZnCl_3$ were observed until the SWNT structure was destroyed (Figure 5l). Even after 10 min of electron beam irradiation, the sidewall of the SWNT retained its original structure (Figure 5e), indicating that the observed fusion of the $ChZnCl_3$ is driven by a thermal process rather than through any structural damage. An earlier study on radiation polymerization using $ChZnCl_3$ as a solvent also showed a high radiation stability of this ionic liquid.[49]

(46) Okazaki, T.; Suenaga, K.; Suenaga, K.; Hirahara, K.; Bandow, S.; Iijima, S.; Shinohara, H. *J. Am. Chem. Soc.* **2001**, *123*, 9673–9674.
(47) Hernandez, E.; Meunier, V.; Smith, B. W.; Rurali, R.; Terrones, H.; Nardelli, M. B.; Terrones, M.; Luzzi, D. E.; Charlier, J. C. *Nano Lett.* **2003**, *3*, 1037–1042.
(48) Warner, J. H.; Ito, Y.; Zaka, M.; Ge, L.; Akachi, T.; Okimoto, H.; Porfyrakis, K.; Watt, A. A. R.; Shinohara, H.; Briggs, G. A. D. *Nano Lett.* **2008**, *8*, 2328–2335.
(49) Wu, G.; Liu, Y.; Long, D. *Macromol. Rapid Commun.* **2005**, *26*, 57–61.

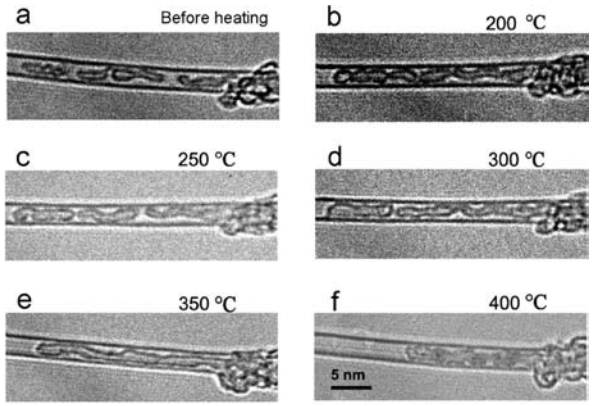

Figure 6. TEM images of an individual $ChZnCl_3$@SWNT (a) before and after annealing in a vacuum for 6 h at (b) 200 °C, (c) 250 °C, (d) 300 °C, (e) 350 °C, and (f) 400 °C.

To investigate thermal heating effects (in reference to the electron beam hearting effects described above) on the packing morphology of $ChZnCl_3$ inside nanotubes, the $ChZnCl_3$@SWNTs were annealed in a vacuum for 6 h at five different temperatures (200 °C, 250 °C, 300 °C, 350 and 400 °C). We fabricated a SiN/Si substrate having channels on the surface to support the $ChZnCl_3$@SWNT sample, and which also allowed TEM observations on precisely the same nanotube after the samples were subjected to heat treatment outside the TEM equipment (Figure 6; cf. Supporting Information, Figure S3).

Before heating, random $ChZnCl_3$ tubes were observed inside the SWNTs (Figure 6a). Subsequent, annealing at 200 °C led to the expansion of the inner ionic liquid tubes, and further heating changed the morphology of encapsulated $ChZnCl_3$ to first zigzag and then continuous tubes (Figure 6b−e). However, after annealing at 400 °C, the inner-tubular structure disappeared, and the ionic liquid transformed into random aggregates (Figure 6f). This temperature-dependent transformation is in good accordance with the melting process observed during the *in situ* TEM electron beam irradiation described earlier.

During the structural transformation of $ChZnCl_3$ ionic liquid nanotubes into the corresponding nanofluids, the first step in the melting process should be associated with the dissociation of the $ChZnCl_3$ solid layer which is in contact with the inner surface of the SWNTs.[50] During the annealing processes, the $ChZnCl_3$ molecules tended to diffuse from the close-packed layer which finally resulted in the $ChZnCl_3$ molecules transforming into liquids that flowed inside the SWNTs. Due to the high viscosity and asymmetrical structure of the ionic liquid, as well as the confined effect of the SWNTs, we propose that the liquid-like $ChZnCl_3$ does not form an ordered-layer structure on the inner surface of SWNTs when the temperature decreases. The transition of $ChZnCl_3$ nanotubes into nanofluids inside SWNTs is therefore an irreversible process.

2.4. Thermal Stability and Doping Effect of Encapsulated Ionic Liquid. The unique melting behavior of $ChZnCl_3$ inside SWNTs prompted us to further investigate the thermal stability of the confined ionic liquid. Thermogravimetric analysis (TGA) was performed on the pure $ChZnCl_3$ ionic liquid and $ChZnCl_3$@SWNTs (Figure 7). We observed that the onset temperature of the thermal decomposition increased by ca. 60 °C when $ChZnCl_3$ was

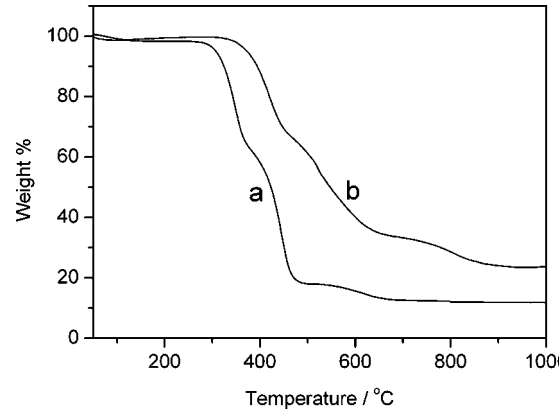

Figure 7. Thermogravimetric analysis (TGA) curves of the (a) pure $ChZnCl_3$ ionic liquid and (b) $ChZnCl_3$@SWNTs.

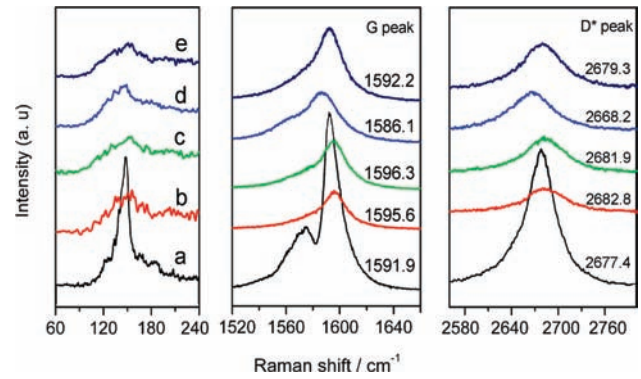

Figure 8. Typical Raman spectra of (a) the pristine SWNTs, (b) $ChZnCl_3$@SWNTs, and $ChZnCl_3$@SWNTs materials after dedoping in a vacuum at different temperatures: (c) 200 °C, (d) 300 °C, (e) 500 °C. The spectra were obtained by using an Ar^+ laser at 2.41 eV.

encapsulated in SWNTs (compare Figure 7a with b). Both the pure $ChZnCl_3$ ionic liquid and $ChZnCl_3$@SWNTs had two main weight-loss regions located at ∼260−375 °C and ∼385−480 °C, and at ∼318−450 °C and ∼485−645 °C, respectively. The first weight loss may be assigned to the decomposition of the organic cation of $ChZnCl_3$ (quaternary ammonium part), and the significant weight reduction in the second region was likely due to the decomposition of the inorganic anion part.[51−53]

Typical Raman spectra of pristine SWNTs and $ChZnCl_3$@SWNTs are presented in Figure 8. At an excitation energy of 2.41 eV (514.5 nm), the pristine SWNTs showed well-known characteristic Raman peaks: the radial breathing mode (RBM) at 148 cm^{-1}, the G band at 1592 cm^{-1}, and the D* mode (an overtone of D peak) at 2677 cm^{-1}. In contrast, the Raman signals of the $ChZnCl_3$@SWNTs were much weaker than those of the pristine SWNTs (Figure 8b). This reduction in intensity can be explained by the encapsulation of $ChZnCl_3$, which induces a change in the structural environment, the local symmetry of SWNTs, and the occurrence of charge transfer. Such encapsulation effects have been reported in several peapod materials and chemically doped SWNTs.[54−60] The peak position of the G-band was upshifted by ca. 5 cm^{-1} upon the encapsula-

(50) Mezger, M.; Schröder, H.; Reichert, H.; Schramm, S.; Okasinski, J. S.; Schöder, S.; Honkimäki, V.; Deutsch, M.; Ocko, B. M.; Ralston, J.; Rohwerder, M.; Stratmann, M.; Dosch, H. *Science* **2008**, *322*, 424–428.

(51) Ohtani, H.; Ishimura, S.; Kumai, M. *Anal. Sci.* **2008**, *24*, 1335–1340.
(52) Domanska, U. *Thermochim. Acta* **2006**, *448*, 19–30.
(53) Busi, S.; Lahtinen, M.; Ropponen, J.; Valkonen, J.; Rissanen, K. *J. Solid State Chem.* **2004**, *177*, 3757–3767.
(54) Takenobu, T.; Takano, T.; Shiraishi, M.; Murakami, Y.; Ata, M.; Kataura, H.; Achiba, Y.; Iwasa, Y. *Nat. Mater.* **2003**, *2*, 683–688.

tion of $ChZnCl_3$, suggesting that encapsulation of $ChZnCl_3$ leads to p-type doping.[61]

To investigate the relationship between thermal stability and the doping effect, the $ChZnCl_3$@SWNTs were annealed in a vacuum for 6 h at three different temperatures (200, 400, and 500 °C) in order to achieve the successive dedoping of $ChZnCl_3$. No obvious peak shifts or intensity drops were observed upon dedoping at 200 °C (compare Figure 8b with c), suggesting that p-type doping is fairly stable due to the high thermal stability of the ionic liquid. A substantial downshift (over 10 cm^{-1}) of G-band and D* mode was observed when the sample was dedoped at 400 °C, indicating that the polarity of the SWNT doping changes from p-type to n-type.[62] The origin of this p-type to n-type transition is likely caused by the difference in the thermal stability of the cation and anion of $ChZnCl_3$. Based on the TGA analysis described earlier, the organic cation of $ChZnCl_3$ may be partly decomposed after heat treatment at 400 °C. This assumption was confirmed by TEM and EDX analysis (data not shown), in which the $ChZnCl_3$ encapsulated SWNTs materials obtained by dedoping at 400 °C showed ClKα and ZnKα peaks, indicating that the inorganic part of $ChZnCl_3$ can survive the heat treatment. In contrast, after dedoping at 500 °C, both TEM and EDX measurements indicated the complete disappearance of the encapsulated $ChZnCl_3$ ionic liquid.

The HRTEM observation also revealed the presence of a unique morphology transformation of the encapsulated $ChZnCl_3$ after annealing at 400 °C (see Figure 6). When the temperature was held at 500 °C for 6 h, all of the encapsulated $ChZnCl_3$ was removed. As a result, the Raman spectra did not show a peak shift which was present in the pristine SWNTs (Figure 8e). The transition from p-type to n-type during the gradual dedoping process was also confirmed by Raman spectroscopy performed with an excitation energy of 1.96 eV (cf. Supporting Information, Figure S4).

3. Conclusion

In summary, we have observed a size-dependent morphology of $ChZnCl_3$ ionic liquids inside SWNTs by HRTEM for the first time. By increasing the diameter of SWNTs, $ChZnCl_3$ can form single-chain, double-helix, zigzag tube, and finally, random tube morphologies. The *in situ* TEM electron beam irradiation and localized TEM observation upon step-by-step annealing have provided insight into the melting process of confined $ChZnCl_3$ ionic liquid. The diameter selective and tunable charge transfer effects between $ChZnCl_3$ and SWNTs were confirmed based on the photoluminescence and Raman spectroscopy. Considering the versatility and unique electronic properties of ionic liquids, and the observed multiform morphology and unique melting process of the ionic liquid inside SWNTs, RTILs are good candidates for elucidating phase behaviors of liquids in confined systems and for fabricating nanotube-based transistors. The present study will hopefully stimulate new experimental and theoretical work for the further understanding of the microstructure and phase behavior of ionic liquids under confinement and lead to new insights for improving the performance of ionic liquids in catalysts, lubricants, fuels, and solar cells.

4. Experimental Section

Materials and Synthesis. A quaternary ammonium based ionic liquid $[Me_3NC_2H_4OH]^+[ZnCl_3]^-$ ($ChZnCl_3$) was prepared by mixing choline chloride and $ZnCl_2$ in a molar ratio of 1:1 at 90 °C according to a method previously described in the literature.[63] SWNTs were synthesized by the enhanced direct injection pyrolytic synthesis (e-DIPS),[64,65] and the raw SWNT products were subsequently annealed in a vacuum at 1200 °C for 24 h in order to remove residual Fe catalyst nanoparticles and amorphous carbon impurities. Before the encapsulation, the SWNTs were heated under dry air flow at 550 °C for 30 min to remove the end-cap. Open-ended SWNTs and anhydrous $ChZnCl_3$ were separately loaded and vacuum-sealed (10^{-7} Torr) in an H-type quartz tube. After mixing these together at 200 °C in a vacuum, the mixture was kept at 200 °C for 72 h. At this temperature, $ChZnCl_3$ melted and was encapsulated within the interior channel of the SWNTs. The as-prepared products were washed with methanol to remove any $ChZnCl_3$ adsorbed on the outer surface of the SWNTs and then dried at 80 °C in a vacuum for 12 h, which provided the final product: $ChZnCl_3$ encapsulated in SWNTs (referred to as $ChZnCl_3$@SWNTs). The filling of $ChZnCl_3$ into tip-closed SWNTs was carried out under the same conditions as a control experiment, and the existence of $ChZnCl_3$ in the exterior of SWNTs was excluded by TEM and EDX analysis (cf. Supporting Information, Figure S5).

Photoluminescence Spectroscopy. Photoluminescence (PL) measurements were performed using a Shimadzu NIR-PL system (CNT-RF) equipped with a liquid-N_2-cooled InGaAs detector array. A slit width of 20 nm was used for both excitation and emission. Excitation light was generated by a Xenon arc lamp. The dispersed solutions of pristine SWNTs and $ChZnCl_3$@SWNTs were prepared with a ratio of 0.1 mg nanotube/10 mg SDBS/10 mL D_2O and then homogenized in a sonic bath for 30 min, which was followed by vigorous sonication using an ultrasonic disintegrator for 2 h to debundle the SWNTs. The sample was centrifuged with a swing-bucket rotor (S52ST- Hitachi Koki) at 52000 rpm for 2 h. The upper 80% of the supernatant was then decanted and used for the optical measurements.

Morphology Characterization. Transmission electron microscopy (TEM) and energy dispersive X-ray (EDX) spectroscopy measurements were performed using a JEOL JEM 2100F microscope equipped with a superatmospheric thin-window X-ray detector. TEM images were acquired at an electron acceleration voltage of 80 keV. The samples for TEM observation were prepared by depositing a drop of the nanotube hexane suspension onto commercially available carbon-coated copper grids or onto homemade channeled SiN/Si substrates. Details on the fabrication of the SiN/Si substrate are shown in Figure S2, Supporting Information.

(55) Dettlaff-Weglikowska, U.; Skkalov, V.; Graupner, R.; Jhang, S. H.; Kim, B. H.; Lee, H. J.; Ley, L.; Park, Y. W.; Berber, S.; Tomnek, D.; Roth, S. *J. Am. Chem. Soc.* **2005**, *127*, 5125–5131.
(56) Kim, K. K.; Bae, J. J.; Park, H. K.; Kim, S. M.; Geng, H.-Z.; Park, K. A.; Shin, H.-J.; Yoon, S.-M.; Benzyad, A.; Choi, J.-Y.; Lee, Y. H. *J. Am. Chem. Soc.* **2008**, *130*, 12757–12761.
(57) Takenobu, T.; Takano, T.; Shiraishi, M.; Murakami, Y.; Ata, M.; Kataura, H.; Achiba, Y.; Iwasa, Y. *Nat. Mater.* **2003**, *2*, 683–688.
(58) Anglaret, E.; Dragin, F.; Pnicaud, A.; Martel, R. *J. Phys. Chem. B* **2006**, *110*, 3949–3954.
(59) Moonoosawmy, K. R.; Kruse, P. *J. Am. Chem. Soc.* **2008**, *130*, 13417–13424.
(60) Ilie, A.; Bendall, J. S.; Roy, D.; Philp, E.; Green, M. L. H. *J. Phys. Chem. B* **2006**, *110*, 13848–13857.
(61) Zhou, W.; Vavro, J.; Nemes, N. M.; Fischer, J. E.; Borondics, F.; Kamaràs, K. *Phy. Rev. B* **2005**, *71*, 2054231−6.
(62) Shim, M.; Ozel, T.; Gaur, A.; Wang, C. *J. Am. Chem. Soc.* **2006**, *128*, 7522–7530.
(63) Abbott, A. P.; Capper, G.; Davis, D. L.; Munro, H. L.; Rasheed, R. K.; Tambyrajah, V. *Chem. Commun.* **2001**, 2010–2011.
(64) Saito, T.; Xu, W.; Ohshima, S.; Ago, H.; Yumura, M.; Iijima, S. *J. Phys. Chem. B* **2006**, *110*, 5849–5853.
(65) Saito, T.; Ohshima, S.; Okazaki, T.; Ohmori, S.; Yumura, M.; Iijima, S. *J. Nanosci. Nanotechnol.* **2008**, *8*, 6153–6157.

Thermal Stability Analysis and Raman Spectroscopy. Thermogravimetric analysis (TGA) was carried out using a Shimadzu TA-60 thermal analysis system under a flowing nitrogen atmosphere at a scan rate of 5 °C/min from 50 to 1000 °C. Raman spectra were measured on a Jobin Yvon HR-800 micro-Raman spectrometer with 514.5 nm (2.41 eV) and 633 nm (1.96 eV) excitation sources under air ambient conditions. The nanotube material was used in the form of thick bundles deposited on a silicon substrate, to ensure that the spectra acquired were characteristic of the overall nanotube distribution. For Raman measurements, 10 different locations for each sample were observed in order to obtain the average Raman profile.

Acknowledgment. This work was supported by Grant-in-Aids for Specific Area Research (No. 19084008) on Carbon Nanotube Nano-Electronics and for Scientific Research A (No.19205003) of MEXT, Japan. S.C. is grateful for the Postdoctoral Fellowship for Foreign Researchers from the Japan Society for Promotion of Science and the Grants-in-Startup for the President Scholarship Winner from the Chinese Academy of Sciences. We also thank Professors H.Sawa and E.Nishibori (Nagoya University) for their help on X-ray diffraction measurements.

Supporting Information Available: X-ray diffraction patterns of pristine SWNTs and $ChZnCl_3$@SWNTs (Figure S1). A series of TEM images show the movement of a nanobubble inside a SWNT during the melting of $ChZnCl_3$ ionic liquid (Figure S2). Details of the fabrication of SiN/Si substrate and the localized-observation for the same nanotubes after each heat treatment (Figure S3). Typical Raman spectra of the $ChZnCl_3$ encapsulated SWNTs materials obtained by a gradual dedoping process recorded at an excitation energy of 1.96 eV (Figure S4). TEM image and EDX spectrum of the sample obtained by a controlled experiment (Figure S5). This material is available free of charge via the Internet at http://pubs.acs.org.

JA904283D